

1 **Hepatitis C virus infection is inhibited by a non-canonical antiviral signaling**
2 **pathway targeted by NS3-NS4A**

3

4

5 Christine Vazquez^a, Chin Yee Tan^a, and Stacy M. Horner^{a,b,#}

6

7

8 ^aDepartment of Molecular Genetics and Microbiology, Duke University Medical Center,

9 Durham, North Carolina, USA

10 ^bDepartment of Medicine, Duke University Medical Center, Durham, North Carolina,

11 USA

12

13

14 Running Title: HCV blocks a non-canonical antiviral signaling pathway

15

16

17 Abstract count: 173 words

18 Text count: 6275 words

19

20

21 #Address correspondence to Stacy M. Horner, stacy.horner@duke.edu

22 **Abstract**

23 The hepatitis C virus (HCV) NS3-NS4A protease complex is required for viral
24 replication and is the major viral innate immune evasion factor. NS3-NS4A evades
25 antiviral innate immunity by inactivating several proteins, including MAVS, the signaling
26 adaptor for RIG-I and MDA5, and Riplet, an E3 ubiquitin ligase that activates RIG-I. Here,
27 we identified a Tyr-16-Phe (Y16F) change in the NS4A transmembrane domain that
28 prevents NS3-NS4A targeting of Riplet but not MAVS. This Y16F substitution reduces
29 HCV replication in Huh7 cells, but not in Huh-7.5 cells, known to lack RIG-I signaling.
30 Surprisingly, deletion of RIG-I in Huh7 cells did not restore Y16F viral replication. Rather,
31 we found that Huh-7.5 cells lack Riplet expression and that addition of Riplet to these
32 cells reduced HCV Y16F replication. In addition, IRF3 deletion in Huh7 cells was sufficient
33 to restore HCV Y16F replication, and the Y16F protease lacked the ability to prevent IRF3
34 activation or interferon induction. Taken together, these data reveal that the NS4A Y16
35 residue regulates a non-canonical Riplet-IRF3-dependent, but RIG-I-MAVS-independent,
36 signaling pathway that limits HCV infection.

37

38

39 **Importance**

40 The HCV NS3-NS4A protease complex facilitates viral replication by cleaving and
41 inactivating the antiviral innate immune signaling proteins MAVS and Riplet, which are
42 essential for RIG-I activation. NS3-NS4A therefore prevents IRF3 activation and
43 interferon induction during HCV infection. Here, we uncover an amino acid residue within
44 the NS4A transmembrane domain that is essential for inactivation of Riplet, but does not
45 affect MAVS cleavage by NS3-NS4A. Our study reveals that Riplet is involved in a RIG-
46 I- and MAVS-independent signaling pathway that activates IRF3 and that this pathway is
47 normally inactivated by NS3-NS4A during HCV infection. Our study selectively uncouples
48 these distinct regulatory mechanisms within NS3-NS4A and defines a new role for Riplet
49 in the antiviral response to HCV. As Riplet is known to be inhibited by other RNA viruses,
50 such as such influenza A virus, this innate immune signaling pathway may also be
51 important in controlling other RNA virus infections.

52

53

54 **Introduction**

55 Hepatitis C virus (HCV) is a positive-sense, singled-stranded RNA virus that infects
56 over 70 million people worldwide, with up to 80% of infected individuals developing
57 chronic infection (1). The recent development of direct-acting antivirals for HCV has
58 dramatically improved successful treatment of HCV infection (2). However, many HCV-
59 infected individuals are asymptomatic and thus unaware of their HCV status until
60 secondary manifestations, such as liver cirrhosis and hepatocellular carcinoma, arise
61 decades later. Notably, although the current direct-acting antivirals treat HCV-induced
62 disease, they do not always prevent re-infection in cured individuals. Therefore, there is
63 an urgent need for future studies into the development of a vaccine to reduce the global
64 burden of HCV infection (3).

65 Several factors contribute to the ability of HCV to establish a chronic infection,
66 including its ability to evade detection and dysregulate the host antiviral innate immune
67 response through the actions of the HCV NS3-NS4A protease complex (4). The NS3-
68 NS4A protease is a protein complex formed between NS3, which contains protease and
69 helicase domains, and NS4A. NS4A is a 54 amino acid protein that contains an N-terminal
70 transmembrane domain, an NS3 interacting domain, and a C-terminal acidic domain (5).
71 The NS4A transmembrane domain anchors NS3 to membranes (6) and mediates NS4A
72 dimerization (7). NS3-NS4A has diverse functions in the HCV life cycle, with roles in HCV
73 RNA replication, viral assembly, and innate immune evasion (reviewed in (8))(9). The
74 mechanisms that regulate these diverse functions of NS3-NS4A are not completely
75 understood. However, it is known that NS4A directs the protease complex to distinct
76 intracellular membranes to perform some of these functions: the ER for viral replication;

77 and mitochondria and mitochondrial-ER contact sites (often referred to as mitochondrial-
78 associated ER membranes (MAM)) for immune evasion (10-14).

79 Antiviral innate immune signaling against HCV can be initiated by the RNA sensor
80 proteins RIG-I and MDA5 (15-17). RIG-I is directly activated by multiple ubiquitination
81 events by E3 ubiquitin ligases, namely TRIM25 and Riplet, which binds to and adds K63-
82 linked ubiquitin chains to RIG-I, but not MDA5 (18-21). Once activated, RIG-I and MDA5
83 signal to the adaptor protein MAVS to drive a signal transduction cascade that induces
84 the phosphorylation of IRF3 and then the transcriptional induction of interferon (IFN)- β .
85 HCV infected can also be sensed by TLR3, which signals via TRIF and IRF3 to induce
86 antiviral innate immunity (22). During HCV infection, NS3-NS4A cleaves and/or
87 inactivates MAVS (10, 12, 23, 24), TRIF (25) and Riplet (19) to block IRF3 activation (26).

88 Here, we aimed to uncouple the roles of NS3-NS4A in replication and immune
89 evasion. We focused on the NS4A transmembrane domain and found a residue, Y16,
90 that regulates differential inactivation of MAVS and Riplet, revealing a new branch of
91 innate immune signaling that controls HCV infection.

92

93 **Results**

94 **A Y16F substitution in NS4A disrupts replication of an HCV subgenomic replicon** 95 **in Huh7 cells, but not in Huh-7.5 cells.**

96 The transmembrane domain of NS4A contains two aromatic amino acids: a
97 tryptophan at position 3 (W3) and a tyrosine at position 16 (Y16) (**Fig. 1A**). These two
98 aromatic amino acids, which are conserved in all sequenced HCV strains in the Los
99 Alamos HCV sequence database ((42) and **Fig. 1A**), are located at each end of the NS4A

100 transmembrane domain at the lipid bilayer interface (5, 7). Interestingly, aromatic residues
101 at the termini of transmembrane domains are often important for positioning membrane
102 proteins within lipid bilayers (43-45). Therefore, we hypothesized that these residues may
103 play a role in the proper localization and/or function of the NS3-NS4A protease complex
104 during HCV infection. While both the W3 and the Y16 residues in NS4A are conserved
105 across the eight known HCV genotypes, we chose to focus specifically on the Y16 residue
106 (**Fig. 1A**), with the goal of uncoupling the function of Y16 in HCV replication from targeting
107 of innate immune substrates, such as MAVS and Riplet. As a prior study found that a
108 Y16A substitution inhibited HCV replication (7), we made the more conservative
109 phenylalanine mutation (Y16F) to maintain aromaticity at this position. Here, we analyzed
110 the role of this amino acid in regulating HCV replication and innate immune regulation by
111 NS3-NS4A.

112 To determine if the Y16F substitution in NS4A altered HCV replication, we first
113 engineered this amino acid change into an HCV replicon encoding a G418 marker (HCV
114 genotype 1B subgenomic replicon; HP replicon (15)). Following *in vitro* transcription, wild-
115 type (WT) or Y16F HCV replicon RNA was electroporated into either liver hepatoma Huh-
116 7.5 cells, which do not have functional RIG-I signaling due to the T55I mutation (15), or
117 Huh7 cells, which have functional RIG-I signaling. In the Huh-7.5 cells, the number of
118 G418-resistant colonies in the WT versus the Y16F HCV replicon-transduced cells was
119 equivalent, indicating that WT and Y16F replicated similarly. However, in Huh7 cells, the
120 Y16F HCV replicon had a reduced transduction efficiency (~3-fold) compared to the WT
121 HCV replicon (**Fig. 1B**). As control, we also measured the interaction of NS4A WT or
122 Y16F with NS3 by co-immunoprecipitation and found that the Y16F substitution did not

123 alter the interaction of NS4A with NS3, nor the ability of the NS3-NS4A protease to
124 process the NS3-NS4A polyprotein junction (**Fig. 1C**). Together, these data reveal that
125 the Y16F mutation results in reduced HCV replication in Huh7 cells, but not Huh-7.5 cells,
126 suggesting that NS4A Y16F may regulate RIG-I-mediated innate immune signaling to
127 promote HCV immune evasion and replication.

128

129 **RIG-I deletion in Huh7 cells does not restore HCV NS4A Y16F viral replication.**

130 To determine if the Y16F substitution in NS4A specifically altered HCV replication
131 in Huh7 cells during infection, we engineered the NS4A Y16F substitution into the full-
132 length HCV infectious clone (JFH1, genotype 2A (33)). We generated low-passage viral
133 stocks and confirmed that the Y16F mutation was maintained in the resulting virus by
134 PCR amplification of the NS4A region and Sanger sequencing. We then infected Huh-7.5
135 or Huh7 cells with the HCV WT or Y16F virus, harvested protein lysates over a time
136 course of infection, and measured HCV NS5A protein expression by immunoblot. We
137 found that HCV NS5A protein levels were equivalent in Huh-7.5 cells infected with WT or
138 Y16F HCV (**Fig. 2A**). However, in Huh7 cells, the level of NS5A protein from the Y16F
139 virus was reduced as compared to WT HCV (**Fig. 2B**). In addition to RIG-I, there are likely
140 other genetic differences between Huh7 and Huh-7.5 cells. Thus, to determine if RIG-I
141 was the factor accounting for the differential replication observed between WT and Y16F
142 HCV in Huh7 cells versus Huh-7.5 cells, we generated Huh7-RIG-I knockout (KO) cells
143 using CRISPR/Cas9 genome editing. These Huh7-RIG-I KO cells contain a 252
144 nucleotide deletion that removes the start codon, preventing RIG-I protein expression
145 (**Fig. 2C**). To confirm a loss of RIG-I signaling, we infected Huh7-RIG-I KO cells with

146 Sendai virus (SV), a virus known to activate RIG-I signaling(15, 46), and observed no SV-
147 mediated induction of RIG-I protein or signaling to the IFN- β promoter, which was restored
148 upon over-expression of RIG-I (15, 16) (**Fig. 2D**).

149 We next infected these Huh7-RIG-I KO cells with either WT or Y16F HCV and
150 measured HCV NS5A expression from lysates harvested over a time course of infection
151 by immunoblotting. Surprisingly, we found that NS5A protein level from Y16F HCV was
152 not restored to the level of WT in the Huh7-RIG-I KO cells (**Fig. 2E**). We then compared
153 the production of infectious virus from the WT and Y16F viruses in each of these cell lines.
154 In these assays, the supernatants of infected cells were used to infect naïve Huh-7.5 cells
155 to determine the viral titer, which ultimately measures a second round of infection. We
156 found that the while the Y16F virus harvested from Huh-7.5 cells resulted in a somewhat
157 lower level of infectious virus as compared to WT (~40% lower), its level of infectious virus
158 harvested from Huh7 or Huh7-RIG-I KO cells was significantly lower as compared to WT
159 (now ~75% lower) (**Figs. 2F-2H**). Taken together, these data suggest that NS4A Y16
160 regulates a RIG-I-independent signaling pathway that is non-functional in Huh-7.5 cells.

161

162 **HCV NS3-NS4A Y16F retains the ability to cleave MAVS.**

163 As NS4A Y16 is located at the membrane lipid bilayer interface (5, 7), and NS4A
164 membrane interactions regulate the molecular mechanisms by which the NS3-NS4A
165 protease targets substrates (7), we hypothesized that the Y16F substitution in NS4A may
166 regulate NS3-NS4A cleavage of MAVS. To test this, we co-expressed NS3-NS4A with
167 Flag-tagged MAVS and found that both NS3-NS4A WT and Y16F cleaved MAVS, while
168 NS3-NS4A containing a mutation that inactivates the protease active site (S139A; SA)

169 did not (**Fig. 3A**). We also found that MAVS cleavage was similar following HCV WT and
170 Y16F infection in both Huh-7.5 and Huh7 cells (**Fig. 3B**). Together, this reveals that the
171 NS4A Y16F substitution does not alter MAVS cleavage by NS3-NS4A.

172

173 **IRF3 deletion in Huh7 cells restores HCV Y16F replication to the levels of HCV WT.**

174 We next wanted to determine if the signaling pathway that inhibits HCV Y16F
175 replication requires the IFN- β transcription factor IRF3 (reviewed in (47)). We first
176 generated Huh7-IRF3 KO cells using CRISPR/Cas9 genome editing and determined
177 IRF3 expression and function in these cells by sequencing the IRF3 genetic locus,
178 analyzing IRF3 expression by immunoblot, and confirming that loss of IRF3 prevented
179 SV-mediated antiviral signaling to the IFN- β promoter and that this signaling was restored
180 by IRF3 over-expression (**Figs. 4A-4B**). To determine if IRF3 regulates HCV Y16F
181 replication, we infected Huh7 or Huh7-IRF3 KO cells with either HCV WT or Y16F,
182 measured HCV NS5A expression by immunoblot, and measured release of infectious
183 virus by focus forming assay. While the levels of NS5A expression and infectious Y16F
184 virus were reduced relative to the WT in parental Huh7 cells, as before, these levels were
185 restored to that of WT virus in Huh7-IRF3 KO cells (**Figs. 4C-4D**). Together, these data
186 reveal that NS4A Y16 regulates an IRF3-dependent signaling pathway that can inhibit
187 HCV replication.

188

189 **HCV NS3-NS4A Y16F does not block IRF3 activation.**

190 As our data suggested that HCV Y16F replication was inhibited by IRF3-mediated
191 signaling, we hypothesized that NS3-NS4A Y16F would be unable to block IRF3

192 activation. During viral infection, IRF3 is activated by a multi-step process, including
193 phosphorylation by the kinases TBK1 and IKK ϵ , resulting in dimerization, and finally
194 translocation from the cytosol to the nucleus, where it activates transcription of IFN- β (41).
195 Importantly, it is well-known that over-expression of the WT NS3-NS4A protease can
196 block this nuclear translocation of IRF3 in response to virus infection (12, 48). Therefore,
197 we measured the ability of WT or Y16F NS3-NS4A to block the nuclear translocation of
198 GFP-IRF3 in response to SV. GFP-IRF3 translocated to the nucleus in approximately
199 50% of the SV-infected cells, as measured by immunofluorescence assay (**Figs. 5A-5B**).
200 While the NS3-NS4A WT blocked nearly all of this nuclear translocation, NS3-NS4A Y16F
201 did not (**Figs. 5A-5B**), revealing that NS3-NS4A Y16F has a reduced ability to inhibit IRF3
202 activation.

203 To test if NS3-NS4A Y16F similarly did not block IRF3 activation in the context of
204 HCV replication, we utilized the HCV replicon system, which activates RIG-I signaling but
205 prevents the transduction of IRF3 signaling by NS3-NS4A cleavage of MAVS, to prevent
206 HCV or SV-induced innate immune signaling (48). We infected control cells and cells
207 stably expressing either WT or Y16F subgenomic replicons with SV and then measured
208 induction of IFN- β and several ISGs by RT-qPCR. While the WT HCV replicon prevented
209 SV-mediated induction of all ISGs tested, the HCV Y16F replicon did not block induction
210 of IFN- β , IFN- λ , IFITM1, and Viperin, and only partially blocked induction of several other
211 ISGs (**Fig. 5C**). Interestingly, in the Huh7-RIG-I KO cells, GFP-IRF3 translocated to the
212 nucleus in approximately 15%-20% of SV-infected cells, while only being nuclear in less
213 than 10% of mock-infected cells, suggesting that other signaling molecules are capable
214 of activating IRF3 in the absence of RIG-I (**Fig. 5D**). Taken together, these data reveal

215 that the Y16F substitution prevents NS3-NS4A from fully blocking IRF3 activation and
216 signaling in response to viral infection.

217

218 **HCV NS4A Y16F does not target Riplet.**

219 Our data described thus far reveal that NS4A Y16 regulates NS3-NS4A inhibition
220 of IRF3-mediated antiviral signaling. This IRF3-mediated signaling, which limits HCV
221 replication, is RIG-I-independent and MAVS-cleavage independent. Together, these data
222 suggest: (1) that there is a factor that induces signaling to IRF3 that is targeted by NS4A
223 Y16 (and not Y16F), and (2) that this factor is present in Huh7 cells but absent or non-
224 functional in Huh-7.5 cells. NS3-NS4A cleaves and inactivates three known host proteins
225 involved in the IRF3 signaling axis: MAVS, TRIF (the TLR3 signaling adaptor), and Riplet
226 (10, 12, 19, 24, 25, 48). Since we have demonstrated that NS3-NS4A Y16F cleaves
227 MAVS (**Fig. 3**), and it is known that Huh7 cells do not have functional TLR3 signaling (49),
228 we hypothesized that the E3 ubiquitin ligase Riplet may be differentially regulated by NS3-
229 NS4A WT and Y16F. Interestingly, we found that Huh-7.5 cells express reduced levels of
230 Riplet (*RNF135*) mRNA as compared to Huh7 cells (**Fig. 6A**). This low level of Riplet likely
231 renders it incapable of driving signaling. Therefore, we tested if Riplet ectopic expression
232 in Huh-7.5 cells could limit HCV Y16F replication relative to HCV WT. We generated Huh-
233 7.5 cells expressing V5-tagged Riplet (**Figs. 6A-6B**), infected these cells with HCV WT
234 or Y16F, and measured HCV NS5A expression. In Huh-7.5 + Riplet-V5 cells, but not Huh-
235 7.5 cells, HCV Y16F replication was reduced compared to WT (**Fig. 6B**). Similarly, the
236 amount of infectious virus generated in the Huh-7.5 + Riplet-V5 cells or Huh7 cells from
237 the HCV Y16F virus was also much lower than WT (~90% lower in each), but in the Huh-

238 7.5 cells, the level of Y16F virus was still only partially reduced compared to WT, similar
239 to before (~50% lower) (**Fig. 6C, Fig. 2**). We note that the overall levels of HCV replication
240 (both WT and Y16F) in the Huh-7.5 + Riplet-V5 cells were lower than those seen in the
241 parental Huh-7.5 cells, likely due to the higher levels of Riplet expression in these cells
242 (**Fig. 6**) and the known role of Riplet in inhibiting HCV replication (19).

243 To test the role of NS4A Y16 in targeting Riplet, we first examined the localization
244 of over-expressed NS3-NS4A WT or Y16F with HA-tagged Riplet in Huh7 cells by
245 immunofluorescence. Similar to others, we did not detect any major difference in the
246 localization of NS4A WT or Y16F (5). In cells expressing NS3-NS4A WT, we found that
247 Riplet was localized in small, punctate aggregates throughout the cytoplasm, whereas in
248 cells expressing NS3-NS4A Y16F, Riplet was diffusely localized throughout the
249 cytoplasm, similar to that seen in vector-expressing cells and described previously (18)
250 (**Fig. 7A**). We also found that in cells expressing NS3-NS4A WT, but not Y16F, Riplet
251 and NS4A were in close proximity to each other (**Fig. 7A, zoom**), suggesting that NS4A
252 may interact with Riplet in a Y16-dependent manner. Indeed, we found that NS4A alone
253 interacted with Flag-tagged Riplet and that the Y16F mutation reduced this interaction by
254 approximately 70% (**Fig. 7B**). Taken together, these data suggest that the NS4A Y16
255 residue is necessary for the ability of NS3-NS4A to interact with Riplet and to block
256 antiviral innate immune signaling during HCV infection

257

258 **Discussion**

259 Our results identify a new antiviral signaling program regulated by HCV NS3-
260 NS4A. We found that mutation of NS4A Tyr-16 to phenylalanine, in both the context of an

261 HCV subgenomic RNA replicon and in the context of fully infectious HCV, results in
262 reduced viral replication in Huh7 cells, but not in Huh-7.5 cells. We show that both NS3-
263 NS4A WT and Y16F cleave MAVS. Further, we found that Huh-7.5 cells, in addition to
264 lacking RIG-I signaling (15), express low levels of Riplet (**Fig. 6**). Importantly, ectopic
265 expression of Riplet in Huh-7.5 cells resulted in reduced replication of HCV Y16F
266 compared to WT virus. We also found that NS4A WT binds to Riplet, while NS4A Y16F
267 does not bind as well. Taken together, this supports the model that HCV inactivates Riplet
268 to prevent signaling to IRF3 and an antiviral response that can inhibit HCV replication.
269 Our work reveals that the NS3-NS4A Y16 residue plays a critical role in the inactivation
270 of this signaling pathway. Thus, NS4A Y16 regulates an antiviral signaling program
271 activated by a Riplet-IRF3-dependent, but RIG-I-MAVS-independent, signaling axis.

272 We found that HCV containing an NS4A Y16F substitution in two HCV genotypes,
273 either the JFH1 genotype 2A virus or the HP genotype 1B subgenomic replicon, has lower
274 levels of replication than WT in Huh7 cells (**Fig. 1B, Fig. 2A and 2B**), but that both the
275 WT and Y16F viruses have similar levels of replication in Huh-7.5 cells or in Huh7-IRF3
276 KO cells (**Fig. 2B, Figs. 4C-4D**). Although we did find that in experiments that assessed
277 viral titer, the Y16F virus from Huh-7.5 cells had a reduced viral titer as compared to the
278 WT. However, this reduction (~50%) was not as much as that of virus harvested from the
279 Huh7 parental, Huh7-RIG-I KO, or Huh-7.5 + Riplet-V5 cells (~80%). This, along with our
280 replication experiments, suggests that the while the Y16F substitution does not itself
281 directly affect the functions of the HCV protease in replication, including HCV polyprotein
282 processing, NS3 helicase function, or viral assembly and envelopment, the virus with this
283 substitution may still be inhibited by the low, remaining levels of Riplet present in the Huh-

284 7.5 cells that we use to measure the production of infectious virus. Indeed, the viral titers
285 between the WT and Y16F viruses harvested from the Huh7-IRF3 KO cells were similar
286 to each other (**Fig. 4D**). Similar to our findings, Kohlway and colleagues found that the
287 replication of genotype 2A subgenomic replicon (pYSGR-JFH1/GLuc) containing this
288 Y16F substitution was not altered in Huh-7.5 cells (7), while Brass and colleagues did find
289 reduced replication of a Y16F genotype 1B subgenomic replicon (pCon1/SG-Neo(I)/AflIII)
290 in Huh-7.5 cells (5). While it is unclear what mediates the difference in our HCV replication
291 results from those of Brass and colleagues, it is possible that this could be due to
292 differences in the replication fitness of the replicons used or that Huh-7.5 cells from
293 different labs do not have the same expression levels of Riplet. Unfortunately, all of our
294 attempts to use CRISPR to delete Riplet from Huh7 cells were unsuccessful.
295 Nevertheless, as we found that the Y16F substitution does not affect either the interaction
296 of NS4A with NS3, processing of the NS3/NS4A junction, or MAVS cleavage, our results
297 suggest that it has a specific role in targeting NS3-NS4A to Riplet.

298 The mechanisms by which the HCV protease targets and inactivates Riplet are not
299 entirely clear. Riplet is an E3 ubiquitin ligase localized in the cytoplasm that activates RIG-
300 I by both binding and adding K63-linked ubiquitin chains to it (20, 50). While others have
301 concluded that NS3-NS4A cleaves Riplet in the first amino acid of its RING domain
302 resulting in its destabilization (19), we were not able to detect a Riplet cleavage product
303 or a reduction in Riplet protein abundance by immunoblot analysis upon over-expression
304 of NS3-NS4A in cells, although we cannot rule out this possibility. While it is possible that
305 NS3-NS4A inactivation of Riplet via cleavage may result in its destabilization, analogous
306 to how NS3-NS4A cleavage of TRIF accelerates its proteolysis (25), it is also possible

307 that simply the binding of NS3-NS4A to Riplet can inactivate it. Indeed, we did find that
308 the localization of Riplet changed from cytoplasmic to punctate, often near NS4A,
309 following over-expression of NS3-NS4A WT, but not Y16F, which could either represent
310 a differential localization as a result of binding to NS4A to prevent Riplet function or
311 represent cleavage by the WT NS3-NS4A (**Fig. 7A**). Indeed, the dengue virus protease
312 co-factor NS2 (analogous to HCV NS4A) inactivates cGAS simply by binding to it and
313 inducing its autophagic degradation (51). Additionally, the influenza A virus NS1 protein
314 inactivates Riplet by binding to it (37). Therefore, while it is clear that NS3-NS4A
315 inactivates Riplet, further studies are needed to determine the exact mechanisms by
316 which this occurs.

317 While HCV NS4A anchors the NS3-NS4A protease to intracellular membranes (6),
318 the mechanisms by which the Y16F substitution in NS4A would specifically alter Riplet
319 localization and block Riplet signaling are unclear. Similar to others, we did not find that
320 the Y16F substitution altered the localization of NS4A within membranes (5). Since NS4A
321 can bind Riplet in the absence of NS3, it is possible that NS4A Y16 is simply required for
322 Riplet binding, either directly or through other proteins. In fact, as the hydroxyl group of
323 this tyrosine residue in NS4A is positioned such that it interacts with the phospholipid
324 head groups of the membrane bilayer, while a phenylalanine at the position would be
325 missing this hydroxyl group, Y16 may be poised to mediate protein-protein interaction
326 directly with Riplet or with accessory binding proteins (5). We also note that it is possible
327 that phosphorylation of NS4A Y16 could regulate these protein-protein interactions. Thus,
328 NS4A Y16 likely mediates interactions with Riplet to prevent Riplet from interacting with
329 proteins that mediate antiviral innate immune signaling.

330 Our results suggest that HCV activates a Riplet-dependent signaling cascade to
331 IRF3 that is independent of both RIG-I and MAVS. The following pieces of evidence
332 presented within this manuscript support the existence of this pathway: (1) NS3-NS4A
333 WT and Y16F both cleave MAVS (**Fig. 3**), (2) Y16F cannot bind to Riplet as well as WT
334 (**Fig. 7**); (3) NS3-NS4A WT, but not Y16F, blocks SV-mediated IRF3 activation and
335 induction of ISGs (**Fig. 5**); (4) WT and Y16F viruses only grow equivalently to each other
336 in cells that lack both RIG-I and Riplet or lack IRF3 (**Fig. 1-2; Fig. 4**); (5) over-expression
337 of Riplet in cells without RIG-I signaling can reduce Y16F viral replication (**Fig. 6**). While
338 the identification of this RIG-I-MAVS independent signaling cascade that induces IRF3
339 activation and IFN- β was surprising to us, others have shown that infection of RIG-I KO
340 mouse embryonic fibroblasts with vesicular stomatitis virus, known to be sensed by only
341 RIG-I (52), does result in a small induction of IFN- β mRNA, even though other stimuli do
342 not induce IFN- β in these cells (20). Thus, it is possible that in our human Huh7-RIG-I KO
343 cells, ISGs are induced during HCV infection to limit Y16F viral replication. Indeed, we do
344 see a low level of IRF3 nuclear translocation in response to SV in these cells (**Fig. 5D**).
345 Overall, this induction of this Riplet-IRF3 signaling pathway in the absence of RIG-I is
346 likely stimulus-dependent and cell type-dependent.

347 We do not yet know the full identity of this Riplet-IRF3 signaling cascade regulated
348 by NS3-NS4A Y16. We predict that Riplet is either directly adding K63-linked ubiquitin
349 chains to signaling proteins in this pathway or that it interacts with these signaling proteins
350 to activate them, as it does with RIG-I (18, 20). The only known Riplet-interacting protein
351 that is K63-ubiquitinated is RIG-I. Therefore, the Riplet-signaling target is likely not MDA5,
352 because it is not a Riplet substrate (18, 20) and the Y16F protease is capable of cleaving

353 the downstream signaling protein. It could be the IRF3 kinases TBK1 and IKK ϵ or some
354 other unknown upstream factor (53, 54). Future studies are needed to further identify the
355 Riplet-interacting proteins that activate this non-canonical antiviral signaling pathway.

356 Here, we identify a new, non-canonical branch of an antiviral signaling pathway
357 regulated by NS3-NS4A that can inhibit HCV infection. This signaling pathway is driven
358 by Riplet to induce IRF3 activation, and our data suggest that it does not require MAVS.
359 This signaling results in the transcriptional induction of IRF3-regulated genes, including
360 IFN- β and several ISGs. Ultimately, full characterization of this novel pathway may reveal
361 insights into antiviral innate immunity to other RNA viruses, such influenza A virus, which
362 inactivates Riplet (37). In summary, our work identified a specific amino acid in NS4A
363 which uncouples Riplet inactivation from MAVS cleavage and HCV replication.
364 Identification of this residue allowed us to show that Riplet can be regulated independently
365 from RIG-I and MAVS during HCV infection, and that NS3-NS4A regulates a Riplet/IRF3-
366 dependent, RIG-I-MAVS-independent branch of an antiviral signaling pathway that limits
367 HCV infection.

368 **Materials and Methods**

369 **Cell culture.** Huh7 and Huh-7.5 (15) cells (gift of Dr. Michael Gale Jr., University of
370 Washington), as well as 293T cells (ATCC; CRL-3216), were grown at 37°C with 5% CO₂
371 in Dulbecco's modification of eagle's medium (DMEM; Mediatech) supplemented with
372 10% fetal bovine serum (FBS; HyClone), and 25 mM 4-(2-hydroxyethyl)-1-
373 piperazineethanesulfonic acid (HEPES; Thermo Fisher), referred to as complete DMEM
374 (cDMEM). Huh7 and Huh-7.5 cells were verified using the Promega GenePrint STR kit

375 (DNA Analysis Facility, Duke University), and all cells were tested and found to be
376 *Mycoplasma*-free using the LookOut PCR Detection Kit (Sigma).

377

378 **Plasmids and transfections.** These plasmids were used in this study: pEF-NS3, pEF-
379 NS3-NS4A (genotype 1B), pEF-NS3-NS4A S1165A (27); pHCV-HP WT (containing the
380 following 7 amino acid changes: NS3 (P1115L, K1609E), NS4B (Q1737R), NS5A
381 (P2007A, L2198S, S2236P), and NS5B (V2971A)) and pHCV-HP Δ NS5B (28); pEF-Tak-
382 Flag MAVS (12); pCR-BluntII-TOPO (Addgene #41824) (29), pHCas9 (Addgene #41815)
383 (29); pCMV-Renilla and pGL4.74 [hRluc/TK] (Promega); pIFN- β -Luc (30); pEF-Tak-Flag
384 and pEF-Tak Flag RIG-I (31); pEGFP-C1-IRF3 (32); psJFHI-M9 WT (33); pX330
385 (Addgene #42230) (34); pcDNA-Blast (35); pPAX2 and pMD2.G (Addgene #35002 (36);
386 Addgene #12259); pCCSB-Riplet-V5 (Dharmacon: NM_032322.4, cDNA clone
387 MGC161700); pCAGGS-HA-Riplet (37) (Dr. Michaela Gack at the University of Chicago);
388 and pCMV-Flag-IRF3 WT (38). psJFHI-M9 Y16F, pEF-NS3-NS4A Y16F, pHCV-HP-
389 Y16F, were generated by QuikChange site-directed mutagenesis (Stratagene) of psJFHI-
390 M9, pEF-NS3-NS4A, and pHCV-HP. The oligonucleotide sequences used for cloning are
391 listed in Table 1. pEF-Tak Flag-Riplet was generated by InFusion (ClonTech) cloning of
392 pCAGGS-HA-Riplet into pEF-Tak. To generate the RIG-I CRISPR guide RNA plasmids
393 (pCR-BluntII-Topo-sgRIGI-1 and pCR-BluntII-Topo-sgRIGI-2), sgRNA oligonucleotides
394 were annealed and inserted into *Afl*III-digested pCR-BluntII-Topo by Gibson Assembly
395 (New England Biolabs). To generate the IRF3 CRISPR guide RNA plasmids, sgRNA
396 oligonucleotides were annealed and inserted into *Bbs*I-digested pX330. All
397 oligonucleotide sequences are listed in Table 1. The sequences of all plasmids were

398 verified by DNA sequencing and are available upon request. DNA transfections were
399 done using FuGENE6 (Promega) according to manufacturer's instructions.

400

401 **Generation of knock out (KO) cell lines.** Huh7-RIG-I KO cells were generated by
402 CRISPR/Cas9, using two guides targeting the intron before exon 1 (sgRNA 1) and within
403 exon 1 (sgRNA 2) that were designed with the CRISPR design tool (<http://crispr.mit.edu>).

404 pCR-BluntII-Topo-sgRIGI-1 and pCR-BluntII-Topo-sgRIGI-2, along with phCas9, which
405 expresses Cas9 and neomycin (G148) resistance, were transfected into Huh7 cells.

406 Huh7-IRF3 KO cells were generated by CRISPR/Cas9 using a single guide that targets
407 exon 2 (39). pX330-sgIRF3, along with pcDNA-Blast (which encodes blasticidin

408 resistance), were transfected into Huh7 cells. In both cases, cells were re-plated the day
409 after transfection at limiting dilutions into 15 cm dishes and then incubated with cDMEM

410 containing either 0.4 mg/ml geneticin (G418; Life Technologies) for 5 days or 0.2 µg/ml
411 blasticidin for 3 days. Individual cell clones were then selected and expanded. Isolated

412 clones were screened for either RIG-I or IRF3 protein expression by immunoblot.
413 Genomic DNA was isolated from candidate RIG-I or IRF3 KO cell clones using the

414 QuickExtract DNA extraction solution (Epicentre). Genomic DNA isolated from the RIG-I
415 or IRF3 KO cell clones was then amplified by PCR using primers spanning exon 1 for

416 RIG-I or exon 2 for IRF3 (see Table 1). The resulting amplicons were cloned into pCR4-
417 TOPO TA (Invitrogen) and Sanger sequenced. For RIG-I, all five of the sequenced

418 genomic DNA clones had the start codon and exon 1 removed (four clones: 252 bp
419 deletion and 1 clone: 250 bp deletion). For IRF3, all five of the clones sequenced had a

420 4 bp deletion at the beginning of exon 2 that causes a frame shift resulting in a premature
421 stop codon within exon 2.

422

423 **Generation of Huh-7.5 + Riplet-V5 cells.** To generate Riplet-V5 expressing lentivirus,
424 293T cells were transfected with pCCSB-Riplet-V5, psPAX2, and pMD2.G. Supernatant
425 was harvested at 48 hours post-transfection and filtered through a 0.45 μm filter. Huh-7.5
426 cells were then infected with the Riplet-V5 lentivirus (500 μl per well of a 6-well plate),
427 and the next day virus was removed and replaced with cDMEM with 0.2 $\mu\text{g}/\text{ml}$ blasticidin
428 until mock-transduced cells died (3-4 days). Blasticidin-resistant cells were harvested as
429 pools, and cells were verified as transduced by immunoblot for Riplet-V5 and RT-qPCR
430 analysis for *RNF135* (Riplet).

431

432 **HCV replicons.** RNA was *in vitro* transcribed (MEGAscript T7 transcription kit; Thermo
433 Fisher) from *Scal*-digested HP-HCV replicon plasmid DNA, either WT, Y16F, or ΔNS5B .
434 The *in vitro* transcribed RNA was treated with DNase (Thermo Fisher), purified by phenol-
435 chloroform extraction, and integrity verified on a denaturing gel. For electroporation, 1 μg
436 of HCV replicon RNA was mixed with 4×10^6 Huh7 or Huh-7.5 cells in cold 1X phosphate
437 buffered saline (PBS) in a 4 mm cuvette and then electroporated at 960 μF and 250 V
438 with a Gene Pulser Xcell system (Bio-Rad). Electroporated cells were plated into 10 cm
439 plates at 2×10^5 , 2×10^4 , 2×10^3 cells per dish, along with 2×10^5 cells that had been
440 electroporated with ΔNS5B RNA. Four hours post electroporation, cells were washed
441 three times with 1X PBS and then once with cDMEM. At twenty-four hours post
442 electroporation, media was changed to cDMEM supplemented with 0.4 mg/ml G418.

443 Following three weeks of G418 selection, cells were fixed and stained with crystal violet
444 in 20% methanol. Colonies from triplicate plates were counted to determine the relative
445 transduction efficiency, expressed as the percentage of Y16F colonies that were stably
446 transduced relative to WT. Huh7-HP WT and Huh7-HP Y16F replicon cell lines were
447 generated by isolating and expanding single clones. The presence of the HCV replicon
448 was determined by sequencing the NS4A-containing region following cDNA synthesis on
449 extracted RNA (RNeasy RNA extraction kit, Qiagen) and PCR amplification of the NS4A
450 region. Oligonucleotides used for PCR and sequencing are listed in Table 1.

451

452 **HCV stock generation and infections.** HCV JFH1-M9 WT and Y16F virus stocks were
453 generated as described previously (33). The sequence of the virus at NS4A was
454 confirmed after each passage by sequencing nested PCR products from generated cDNA
455 using the oligonucleotides indicated in Table 1, as previously described (9). For HCV
456 infections, cells were incubated in a low volume of serum-free DMEM containing virus at
457 a multiplicity of infection (MOI) of 0.3 for 2-3 hours, after which cDMEM was replenished.
458 To quantify virus, cellular supernatants were analyzed by focus forming assay.

459

460 **Focus forming assay.** To measure HCV titer, supernatants from infected cells were
461 serially diluted and then used to infect naïve Huh-7.5 cells in triplicate wells of a 48-well
462 plate for 3 hours. At 48 hours post infection, cells were washed with PBS and fixed with
463 4% methanol-free paraformaldehyde (Sigma) for 30 minutes, and then washed again with
464 PBS. Cells were then permeabilized (0.2% Triton-X-100 (Sigma) in PBS), blocked (10%
465 FBS in PBS), and immunostained with a mouse anti-HCV NS5A antibody (1:500).

466 Infected cells were visualized following incubation with horseradish peroxidase (HRP)-
467 conjugated secondary mouse antibody (1:500; Jackson ImmunoResearch) and VIP
468 Peroxidase Substrate Kit (Vector Laboratories). Foci were counted at 10X magnification,
469 and viral titer was calculated using the following formula: (dilution factor x number of foci
470 x 1000)/volume of infection (in μ l), resulting in units of focus forming units / ml (FFU/ml).

471

472 **Immunoblotting.** Cells were lysed in a modified RIPA buffer (10 mM Tris pH 7.5, 150
473 mM NaCl, 0.5% sodium deoxycholate, 1% Triton X-100) supplemented with protease
474 inhibitor cocktail (Sigma) and phosphatase inhibitor cocktail (Millipore), and post-nuclear
475 supernatants were harvested by centrifugation. Protein concentration was determined by
476 Bradford assay, and 10 μ g quantified protein was resolved by SDS/PAGE, transferred to
477 either PVDF (for NS4A) or nitrocellulose membranes using either the Trans-Blot Turbo
478 System (BioRad) or a wet system (BioRad), and blocked with either 3% bovine serum
479 albumin (Sigma) in PBS with 0.1% Tween (PBS-T) or 10% FBS in PBS-T. Membranes
480 were probed with specific antibodies against proteins of interest, washed 3X with PBS-T,
481 and incubated with species-specific HRP-conjugated antibodies (Jackson
482 ImmunoResearch, 1:5000), washed again 3X with PBS-T, and treated with Clarity
483 enhanced chemiluminescence substrate (BioRad). Membranes were then imaged on X-
484 ray film or by using a LICOR Odyssey FC. Immunoblots imaged using the LICOR
485 Odyssey FC were quantified with ImageStudio software, and raw values of the protein of
486 interest were normalized to those of controls (either Tubulin or GAPDH, as indicated). For
487 immunoblots developed on film, Fiji was used (40). ImageStudio and Fiji give similar
488 quantification results when compared directly.

489

490 **Immunoprecipitation.** Quantified protein (between 80-160 µg) was incubated with
491 protein-specific antibodies (either R anti-HA (Sigma) or anti-NS4A) in PBS at 4°C
492 overnight with head over tail rotation. The lysate/antibody mixture was then incubated
493 with either Protein A (for Flag-Riplet experiments) or Protein G Dynabeads (Invitrogen)
494 for 2 hours. Beads were washed 3X in either PBS or RIPA for immunoprecipitation and
495 eluted in 2X Laemmli Buffer (BioRad) supplemented with 5% 2-mercaptoethanol at 50°C
496 for 5 minutes. Proteins were resolved by SDS/PAGE and subjected to immunoblotting as
497 described above.

498

499 **Immunofluorescence analysis and confocal microscopy.** Huh7 cells in 4-well
500 chamber slides were fixed in 4% formaldehyde, permeabilized with 0.2% Triton-X-100,
501 and immunostained with the following antibodies: mouse anti-HCV NS4A (Genotype 1B,
502 1:100, Virogen), rabbit anti-HA (1:100, Sigma), and rabbit anti-Sendai virus (SV) (1:1000,
503 MBL International). Secondary antibody incubations were done with Alexa Fluor
504 conjugated antibodies (Thermo Fisher) and with Hoescht (Thermo Fisher) for 1 hour.
505 Following antibody incubations, slides were washed with 1X PBS, and mounted with
506 ProLong Gold Antifade mounting medium (Invitrogen). Samples were imaged on a Zeiss
507 780 Upright Confocal using a 63X/1.25 oil objective and the 405, 488, 561, and 633 laser
508 lines with pinholes set to 1 AU for each channel (Light Microscopy Core Facility, Duke
509 University). Imaging analysis was done using Fiji software (40).

510

511 **Antibodies.** Antibodies used for immunoblot and immunofluorescence analysis include:
512 mouse anti-HCV NS4A (Genotype 1B, 1:1000, Virogen), mouse anti-HCV NS3 (Genotype
513 1B, 1:1000, Adipogen), mouse anti-HCV NS5A (Genotype 2A, 1:1000, clone 9e10, gift of
514 Dr. Charles Rice, Rockefeller University), mouse anti-Tubulin (1:5000, Sigma), mouse
515 anti-RIG-I (1:1000, Adipogen), anti-Flag-HRP (1:2500, Sigma), rabbit anti-Flag (1:1000,
516 Sigma), rabbit anti-MAVS (1:1000, Bethyl Laboratories), mouse anti-IRF3 (1:1000, gift
517 from Dr. Michael Gale Jr., University of Washington (41)), mouse anti-V5 (1:1000, Sigma),
518 mouse anti-HA (1:1000, Sigma), rabbit anti-GAPDH (1:1000, Cell Signaling Technology),
519 Hoescht (1:500, Thermo Fisher), Alexa Fluor conjugated secondary antibodies (1:500,
520 Life Technologies), and rabbit anti-SV (1:1000, MBL International).

521

522 **IFN- β promoter luciferase assays.** IFN- β promoter luciferase assays were performed
523 by transfecting cells with pCMV-Renilla or pGL4.74 [hRluc/TK], pIFN- β -Luc, and
524 expression plasmids as indicated. The following day, cells were infected with SV (Cantrell
525 strain; Charles River labs). SV infections were performed in serum-free media at 200
526 hemagglutination units (HAU) for 1 h, after which complete media was replenished. At 20
527 hours post infection, cells were lysed, and a dual luciferase assay was performed
528 (Promega). Values are displayed as relative luciferase units (RLU), which normalizes the
529 Firefly luciferase (IFN- β -Luc) values to Renilla luciferase.

530

531 **Reverse transcription-quantitative PCR (RT-qPCR).** RNA was extracted from cell
532 lysates using the RNeasy RNA extraction kit, and cDNA synthesis was performed on
533 extracted RNA using iScript (BioRad). The resulting cDNA was diluted (either 1:3 or 1:4)

534 in ddH₂O. RT-qPCR analysis was performed using the Power SYBR Green PCR master
535 mix (Thermo Fisher) on the QuantStudio 6 Flex RT-PCR system. The oligonucleotide
536 sequences used for RT-qPCR are listed in Table 1. Heat map analysis was generated
537 using Morpheus Software from the Broad (<https://software.broadinstitute.org/morpheus>).
538 First the $2^{\Delta\Delta Ct}$ values (Comparative Ct Method) were calculated by setting the mock-
539 infected Huh7 sample Ct value as the baseline for each biological replicate. Then, the
540 mean of the SV-infected Huh7 triplicate samples is set to 1, and the relative fold induction
541 for each gene between samples is shown.

542

543 **Statistical Analysis.** Student's unpaired *t* test or one-way ANOVA were implemented for
544 statistical analysis of the data using GraphPad Prism software. Graphed values are
545 presented as mean \pm SD or SEM (*n* = 3 or as indicated); **p* \leq 0.05, ***p* \leq 0.01, and ****p*
546 \leq 0.005.

547

548 **Acknowledgements**

549 We would like to thank the members of the Horner Lab and Dr. Heather Vincent for
550 discussion and review of the manuscript, as well as Dr. Nicholas Barrows, Moonhee Park,
551 Kevin Labagnara, Bianca Lupan, and Jason Willer for assistance with experiments, the
552 Duke University Light Microscopy Core Facility, and the Duke Functional Genomics Core
553 Facility. We also thank the following for reagents: Dr. Charles Rice at Rockefeller
554 University, Dr. Michaela Gack at the University of Chicago, Dr. So Young Kim at the Duke
555 University Functional Genomics Core, Dr. Michael Gale Jr. at the University of
556 Washington, Dr. Adolfo Garcia-Sastre at Mount Sinai School of Medicine, and Dr. Shelton
557 Bradrick and Dr. Mariano Garcia-Blanco at the University of Texas Medical Branch. This

558 work was supported by funds from the National Institutes of Health (NIH): K22AI100935
559 (S.M.H.); R21AI124100 (S.M.H). Additional funding sources include the Burroughs
560 Wellcome Fund (S.M.H); a Duke Bridge Award (S.M.H), and the Ford Foundation (CV).

561

562 **Conflicts of interest**

563 The authors declare that they have no conflicts of interest with the contents of this article.

564 The content is solely the responsibility of the authors and does not necessarily represent
565 the official views of the National Institutes of Health.

566

567 **References**

- 568 1. Global Hepatitis Report 2017. Geneva: World Health Organization; 2017. Licence: CC BY-
569 NC-SA 3.0 IGO.
- 570 2. **Grebely J, Hajarizadeh B, Dore GJ.** 2017. Direct-acting antiviral agents for HCV infection
571 affecting people who inject drugs. *Nat Rev Gastroenterol Hepatol* **14**:641-651.
- 572 3. **Bartenschlager R, Baumert TF, Bukh J, Houghton M, Lemon SM, Lindenbach BD,**
573 **Lohmann V, Moradpour D, Pietschmann T, Rice CM, Thimme R, Wakita T.** 2018.
574 Critical challenges and emerging opportunities in hepatitis C virus research in an era of
575 potent antiviral therapy: Considerations for scientists and funding agencies. *Virus Res.*
576 **248**:53-62.
- 577 4. **Horner SM, Gale M, Jr.** 2013. Regulation of hepatic innate immunity by hepatitis C virus.
578 *Nat. Med.* **19**:879-888.
- 579 5. **Brass V, Berke JM, Montserret R, Blum HE, Penin F, Moradpour D.** 2008. Structural
580 determinants for membrane association and dynamic organization of the hepatitis C virus
581 NS3-4A complex. *Proc. Natl. Acad. Sci. U. S. A.* **105**:14545-14550.
- 582 6. **Wolk B, Sansonno D, Krausslich HG, Dammacco F, Rice CM, Blum HE, Moradpour**
583 **D.** 2000. Subcellular localization, stability, and trans-cleavage competence of the hepatitis
584 C virus NS3-NS4A complex expressed in tetracycline-regulated cell lines. *J. Virol.*
585 **74**:2293-2304.

- 586 7. **Kohlway A, Pirakitikulr N, Barrera FN, Potapova O, Engelman DM, Pyle AM,**
587 **Lindenbach BD.** 2014. Hepatitis C virus RNA replication and virus particle assembly
588 require specific dimerization of the NS4A protein transmembrane domain. *J. Virol.* **88**:628-
589 642.
- 590 8. **Morikawa K, Lange CM, Gouttenoire J, Meylan E, Brass V, Penin F, Moradpour D.**
591 2011. Nonstructural protein 3-4A: the Swiss army knife of hepatitis C virus. *J. Viral Hepat.*
592 **18**:305-315.
- 593 9. **Roder AE, Vazquez C.** 2019. The acidic domain of the hepatitis C virus NS4A protein is
594 required for viral assembly and envelopment through interactions with the viral E1
595 glycoprotein. **15**:e1007163.
- 596 10. **Li XD, Sun L, Seth RB, Pineda G, Chen ZJ.** 2005. Hepatitis C virus protease NS3/4A
597 cleaves mitochondrial antiviral signaling protein off the mitochondria to evade innate
598 immunity. *Proc. Natl. Acad. Sci. U. S. A.* **102**:17717-17722.
- 599 11. **Moradpour D, Penin F, Rice CM.** 2007. Replication of hepatitis C virus. *Nat Rev Microbiol*
600 **5**:453-463.
- 601 12. **Loo YM, Owen DM, Li K, Erickson AK, Johnson CL, Fish PM, Carney DS, Wang T,**
602 **Ishida H, Yoneyama M, Fujita T, Saito T, Lee WM, Hagedorn CH, Lau DT, Weinman**
603 **SA, Lemon SM, Gale M, Jr.** 2006. Viral and therapeutic control of IFN-beta promoter
604 stimulator 1 during hepatitis C virus infection. *Proc. Natl. Acad. Sci. U. S. A.* **103**:6001-
605 6006.
- 606 13. **Horner SM, Liu HM, Park HS, Briley J, Gale M, Jr.** 2011. Mitochondrial-associated
607 endoplasmic reticulum membranes (MAM) form innate immune synapses and are
608 targeted by hepatitis C virus. *Proc. Natl. Acad. Sci. U. S. A.* **108**:14590-14595.
- 609 14. **Mottola G, Cardinali G, Ceccacci A, Trozzi C, Bartholomew L, Torrisi MR, Pedrazzini**
610 **E, Bonatti S, Migliaccio G.** 2002. Hepatitis C virus nonstructural proteins are localized in
611 a modified endoplasmic reticulum of cells expressing viral subgenomic replicons. *Virology*
612 **293**:31-43.
- 613 15. **Sumpter R, Jr., Loo YM, Foy E, Li K, Yoneyama M, Fujita T, Lemon SM, Gale M, Jr.**
614 2005. Regulating intracellular antiviral defense and permissiveness to hepatitis C virus
615 RNA replication through a cellular RNA helicase, RIG-I. *J. Virol.* **79**:2689-2699.
- 616 16. **Saito T, Hirai R, Loo YM, Owen D, Johnson CL, Sinha SC, Akira S, Fujita T, Gale M,**
617 **Jr.** 2007. Regulation of innate antiviral defenses through a shared repressor domain in
618 RIG-I and LGP2. *Proc. Natl. Acad. Sci. U. S. A.* **104**:582-587.

- 619 17. **Israelow B, Narbus CM, Sourisseau M, Evans MJ.** 2014. HepG2 cells mount an
620 effective antiviral interferon-lambda based innate immune response to hepatitis C virus
621 infection. *Hepatology* **60**:1170-1179.
- 622 18. **Oshiumi H, Matsumoto M, Hatakeyama S, Seya T.** 2009. Riplet/RNF135, a RING finger
623 protein, ubiquitinates RIG-I to promote interferon-beta induction during the early phase of
624 viral infection. *J. Biol. Chem.* **284**:807-817.
- 625 19. **Oshiumi H, Miyashita M, Matsumoto M, Seya T.** 2013. A distinct role of Riplet-mediated
626 K63-Linked polyubiquitination of the RIG-I repressor domain in human antiviral innate
627 immune responses. *PLoS Pathog.* **9**:e1003533.
- 628 20. **Cadena C, Ahmad S, Xavier A, Willemsen J, Park S, Park JW, Oh SW, Fujita T, Hou
629 F, Binder M, Hur S.** 2019. Ubiquitin-Dependent and -Independent Roles of E3 Ligase
630 RIPLET in Innate Immunity. *Cell*.
- 631 21. **Gack MU, Shin YC, Joo CH, Urano T, Liang C, Sun L, Takeuchi O, Akira S, Chen Z,
632 Inoue S, Jung JU.** 2007. TRIM25 RING-finger E3 ubiquitin ligase is essential for RIG-I-
633 mediated antiviral activity. *Nature* **446**:916-920.
- 634 22. **Wang N, Liang Y, Devaraj S, Wang J, Lemon SM, Li K.** 2009. Toll-like receptor 3
635 mediates establishment of an antiviral state against hepatitis C virus in hepatoma cells. *J.
636 Virol.* **83**:9824-9834.
- 637 23. **Bellecave P, Sarasin-Filipowicz M, Donze O, Kennel A, Gouttenoire J, Meylan E,
638 Terracciano L, Tschopp J, Sarrazin C, Berg T, Moradpour D, Heim MH.** 2010.
639 Cleavage of mitochondrial antiviral signaling protein in the liver of patients with chronic
640 hepatitis C correlates with a reduced activation of the endogenous interferon system.
641 *Hepatology* **51**:1127-1136.
- 642 24. **Meylan E, Curran J, Hofmann K, Moradpour D, Binder M, Bartenschlager R, Tschopp
643 J.** 2005. Cardif is an adaptor protein in the RIG-I antiviral pathway and is targeted by
644 hepatitis C virus. *Nature* **437**:1167-1172.
- 645 25. **Li K, Foy E, Ferreon JC, Nakamura M, Ferreon AC, Ikeda M, Ray SC, Gale M, Jr.,
646 Lemon SM.** 2005. Immune evasion by hepatitis C virus NS3/4A protease-mediated
647 cleavage of the Toll-like receptor 3 adaptor protein TRIF. *Proc. Natl. Acad. Sci. U. S. A.*
648 **102**:2992-2997.
- 649 26. **Foy E, Li K, Wang C, Sumpter R, Jr., Ikeda M, Lemon SM, Gale M, Jr.** 2003. Regulation
650 of interferon regulatory factor-3 by the hepatitis C virus serine protease. *Science*
651 **300**:1145-1148.

- 652 27. **Johnson CL, Owen DM, Gale M, Jr.** 2007. Functional and therapeutic analysis of
653 hepatitis C virus NS3.4A protease control of antiviral immune defense. *J. Biol. Chem.*
654 **282**:10792-10803.
- 655 28. **Sumpter R, Jr., Wang C, Foy E, Loo YM, Gale M, Jr.** 2004. Viral evolution and interferon
656 resistance of hepatitis C virus RNA replication in a cell culture model. *J. Virol.* **78**:11591-
657 11604.
- 658 29. **Mali P, Yang L, Esvelt KM, Aach J, Guell M, DiCarlo JE, Norville JE, Church GM.**
659 2013. RNA-guided human genome engineering via Cas9. *Science* **339**:823-826.
- 660 30. **Fredericksen B, Akkaraju GR, Foy E, Wang C, Pflugheber J, Chen ZJ, Gale M, Jr.**
661 2002. Activation of the interferon-beta promoter during hepatitis C virus RNA replication.
662 *Viral Immunol.* **15**:29-40.
- 663 31. **Yoneyama M, Kikuchi M, Natsukawa T, Shinobu N, Imaizumi T, Miyagishi M, Taira**
664 **K, Akira S, Fujita T.** 2004. The RNA helicase RIG-I has an essential function in double-
665 stranded RNA-induced innate antiviral responses. *Nat. Immunol.* **5**:730-737.
- 666 32. **Basler CF, Mikulasova A, Martinez-Sobrido L, Paragas J, Muhlberger E, Bray M,**
667 **Klenk HD, Palese P, Garcia-Sastre A.** 2003. The Ebola virus VP35 protein inhibits
668 activation of interferon regulatory factor 3. *J. Virol.* **77**:7945-7956.
- 669 33. **Aligeti M, Roder A, Horner SM.** 2015. Cooperation between the Hepatitis C Virus p7 and
670 NS5B Proteins Enhances Virion Infectivity. *J. Virol.* **89**:11523-11533.
- 671 34. **Cong L, Ran FA, Cox D, Lin S, Barretto R, Habib N, Hsu PD, Wu X, Jiang W, Marraffini**
672 **LA, Zhang F.** 2013. Multiplex genome engineering using CRISPR/Cas systems. *Science*
673 **339**:819-823.
- 674 35. **Kennedy EM, Whisnant AW, Kornepati AV, Marshall JB, Bogerd HP, Cullen BR.**
675 2015. Production of functional small interfering RNAs by an amino-terminal deletion
676 mutant of human Dicer. *Proc. Natl. Acad. Sci. U. S. A.* **112**:E6945-6954.
- 677 36. **Pfisterer U, Kirkeby A, Torper O, Wood J, Nelander J, Dufour A, Bjorklund A,**
678 **Lindvall O, Jakobsson J, Parmar M.** 2011. Direct conversion of human fibroblasts to
679 dopaminergic neurons. *Proc. Natl. Acad. Sci. U. S. A.* **108**:10343-10348.
- 680 37. **Rajsbaum R, Albrecht RA, Wang MK, Maharaj NP, Versteeg GA, Nistal-Villan E,**
681 **Garcia-Sastre A, Gack MU.** 2012. Species-specific inhibition of RIG-I ubiquitination and
682 IFN induction by the influenza A virus NS1 protein. *PLoS Pathog.* **8**:e1003059.
- 683 38. **Hiscott J.** 2007. Triggering the innate antiviral response through IRF-3 activation. *J. Biol.*
684 *Chem.* **282**:15325-15329.

- 685 39. **Shalem O, Sanjana NE, Hartenian E, Shi X, Scott DA, Mikkelsen T, Heckl D, Ebert**
686 **BL, Root DE, Doench JG, Zhang F.** 2014. Genome-scale CRISPR-Cas9 knockout
687 screening in human cells. *Science* **343**:84-87.
- 688 40. **Schindelin J, Arganda-Carreras I, Frise E, Kaynig V, Longair M, Pietzsch T,**
689 **Preibisch S, Rueden C, Saalfeld S, Schmid B, Tinevez JY, White DJ, Hartenstein V,**
690 **Eliceiri K, Tomancak P, Cardona A.** 2012. Fiji: an open-source platform for biological-
691 image analysis. *Nat Methods* **9**:676-682.
- 692 41. **Rustagi A, Gale M, Jr.** 2014. Innate antiviral immune signaling, viral evasion and
693 modulation by HIV-1. *J. Mol. Biol.* **426**:1161-1177.
- 694 42. **Kuiken C, Yusim K, Boykin L, Richardson R.** 2005. The Los Alamos hepatitis C
695 sequence database. *Bioinformatics* **21**:379-384.
- 696 43. **Braun P, von Heijne G.** 1999. The aromatic residues Trp and Phe have different effects
697 on the positioning of a transmembrane helix in the microsomal membrane. *Biochemistry*
698 **38**:9778-9782.
- 699 44. **de Planque MR, Bonev BB, Demmers JA, Greathouse DV, Koeppe RE, 2nd,**
700 **Separovic F, Watts A, Killian JA.** 2003. Interfacial anchor properties of tryptophan
701 residues in transmembrane peptides can dominate over hydrophobic matching effects in
702 peptide-lipid interactions. *Biochemistry* **42**:5341-5348.
- 703 45. **Wimley WC, White SH.** 1996. Experimentally determined hydrophobicity scale for
704 proteins at membrane interfaces. *Nat. Struct. Biol.* **3**:842-848.
- 705 46. **Saito T, Owen DM, Jiang F, Marcotrigiano J, Gale M, Jr.** 2008. Innate immunity induced
706 by composition-dependent RIG-I recognition of hepatitis C virus RNA. *Nature* **454**:523-
707 527.
- 708 47. **Honda K, Takaoka A, Taniguchi T.** 2006. Type I interferon [corrected] gene induction by
709 the interferon regulatory factor family of transcription factors. *Immunity* **25**:349-360.
- 710 48. **Foy E, Li K, Sumpter R, Jr., Loo YM, Johnson CL, Wang C, Fish PM, Yoneyama M,**
711 **Fujita T, Lemon SM, Gale M, Jr.** 2005. Control of antiviral defenses through hepatitis C
712 virus disruption of retinoic acid-inducible gene-I signaling. *Proc. Natl. Acad. Sci. U. S. A.*
713 **102**:2986-2991.
- 714 49. **Li K, Chen Z, Kato N, Gale M, Jr., Lemon SM.** 2005. Distinct poly(I-C) and virus-activated
715 signaling pathways leading to interferon-beta production in hepatocytes. *J. Biol. Chem.*
716 **280**:16739-16747.

- 717 50. **Gao D, Yang YK, Wang RP, Zhou X, Diao FC, Li MD, Zhai ZH, Jiang ZF, Chen DY.**
 718 2009. REUL is a novel E3 ubiquitin ligase and stimulator of retinoic-acid-inducible gene-1.
 719 PLoS One 4:e5760.
- 720 51. **Aguirre S, Luthra P, Sanchez-Aparicio MT, Maestre AM, Patel J, Lamothe F,**
 721 **Fredericks AC, Tripathi S, Zhu T, Pintado-Silva J, Webb LG, Bernal-Rubio D,**
 722 **Solovyov A, Greenbaum B, Simon V, Basler CF, Mulder LC, Garcia-Sastre A,**
 723 **Fernandez-Sesma A.** 2017. Dengue virus NS2B protein targets cGAS for degradation
 724 and prevents mitochondrial DNA sensing during infection. PLoS Pathog. 2:17037.
- 725 52. **Kato H, Takeuchi O, Sato S, Yoneyama M, Yamamoto M, Matsui K, Uematsu S, Jung**
 726 **A, Kawai T, Ishii KJ, Yamaguchi O, Otsu K, Tsujimura T, Koh CS, Reis e Sousa C,**
 727 **Matsuura Y, Fujita T, Akira S.** 2006. Differential roles of MDA5 and RIG-I helicases in
 728 the recognition of RNA viruses. Nature 441:101-105.
- 729 53. **Fitzgerald KA, McWhirter SM, Faia KL, Rowe DC, Latz E, Golenbock DT, Coyle AJ,**
 730 **Liao SM, Maniatis T.** 2003. IKKepsilon and TBK1 are essential components of the IRF3
 731 signaling pathway. Nat. Immunol. 4:491-496.
- 732 54. **Sharma S, tenOever BR, Grandvaux N, Zhou GP, Lin R, Hiscott J.** 2003. Triggering
 733 the interferon antiviral response through an IKK-related pathway. Science 300:1148-1151.
 734

735
 736
 737
 738
 739

Table 1: Oligonucleotides used for RT-qPCR and cloning

Target	Forward Primer (5'-3')	Reverse Primer (5'-3')
<i>GAPDH</i>	AAGGTGAAGGTCG GAGTCAAC	GGGGTCATTGATGGCAA CAATA
<i>HPRT1</i>	TGACACTGGCAAACAAT GCA	GGTCCTTTTCACCAGCAA GCT
<i>IFNB1</i>	CTTTGCTATTTTCAGACA AGATTCA	GCCAGGAGGTTCTCAAC AAT
<i>IFNL1</i>	CTTCCAAGCCCACCACAA CT	GGCCTCCAGGACCTTCA GC
<i>OAS1</i>	TGTCCAAGGTGGTAAAG GGTG	CCGGCGATTTAAGTATC CTG
<i>IFIT1</i>	TCCTTGGGTTCTCTACA AAT	TTCTCAAAGTCAGCAGCC AGT
<i>IFIT2</i>	CACGCTGTGGCTCATCTG AA	GGCTGGCAAGAATGGAA CA

<i>IFIT3</i>	AGTCTAGTCACTTGGGGA AAC	ATAAATCTGAGCATCTC GAGTC	640
<i>Viperin</i>	TGCCACAATGTGGGTGCT TACAC	CTCAAGGGGCAGCAC AGGAT	741
<i>MxA</i>	TTCAGCACCTGATGGCCT ATC	TGGATGATCAAAGGGA GTGG	742
<i>IFITM1</i>	ACTAGTAGCCGCCCATAG CC	GCACGTGCACTTTATT ATG	743
<i>ISG15</i>	GCGAACTCATCTTTGCCA GTA	CCAGCA TCTTCACCGTCAG	744
<i>RNF135</i>	GGGTGGCAGTAGAGAAG AGC	CCAGAAGAAAAGCCT CCC	745
HCV PCR Outer	TACATGTGTTTAGTCGAG GTT	CAAACAGCCACCAAG AG	746
HCV PCR Inner	CAGGACCATCTGGAGTTC TGG	CTTGCTTGGTGGCTGT G	747
RIG-I KO guide 1	TTTCTTGGCTTTATATATCTTGT GGAAAGGACGAAACACCGG CTAGTGAGGCACAGCCTGCGG G	GACTAGCCTTATTTAACTTGC TATTTCTAGCTCTAAAACCC GCAGGCTGTGCCTCACT AGCC	
RIG-I KO guide 2	TTTCTTGGCTTTATATATCTTGT GGAAAGGACGAAACACCGG GGAGATCTTACCACAAAC CTGGG	GACTAGCCTTATTTAACTTGC TATTTCTAGCTCTAAAACCC AGGTTTGTGGTAAGATCT CCC	
RIG-I PCR	CCGCTAGTTGCACTTTTCG AT	CTTCCCCAGCTTTGAACC TA	
IRF3 KO guide	CCACTGGTGCATATGTTC CC	AAACGGGAACATATGCAC CAGTGGC	
IRF3 PCR	GGGGATGGACCTTGACAG AGT	CCTGAGCCAGTGCTGAC CCT	
pEF-Tak Flag- Riplet	GATGATAAAGCGGCCGC TGCGGGCCTGGGCCT	CTGATCAGCGGGTTTAAA CTTACACCTTTACTTGCT TTATTATCAGGTAATTTCC	
pEF NS4A-HA Y16F	AGCTCTGGCCGCGTTTTG CCTGACAACAG	CTGTTGTCAGGCCAAAACG CGGCCAGAGCT	
pHCV-HP Y16F	CCCGACAGGGAAGTCCT TTCCGGGAGTTC	GAACTCCCGGAAAAGGA CTTCCCTGTCGGG	

748 **Figure Legends**

749 **Figure 1. A Y16F substitution in NS4A disrupts replication of an HCV subgenomic**
750 **replicon in Huh7 cells, but not in Huh-7.5 cells.**

751 **(A)** Amino acid sequence of NS4A, with the Y16 residue starred and indicated in teal.
752 Numbers correspond with the amino acid position within NS4A (aa 1-54) or the full-length
753 HCV polyprotein (aa 1662-1715). Strain names are listed as found in the Los Alamos
754 HCV sequence database. Conserved amino acids are indicated with a dot, while
755 differences are listed. **(B)** Representative images of Huh-7.5 or Huh7 cells electroporated
756 with *in vitro* transcribed HCV subgenomic replicon RNA (HP, genotype 1B; WT or Y16F).
757 Cells were plated in serial dilutions (2×10^5 , 2×10^4 , 2×10^3) and then stained with crystal
758 violet after three weeks of G418 selection. Graphs show the relative transduction
759 efficiency, which denote the % of colonies in Y16F transduced cells relative to WT. Bars
760 indicate mean \pm SEM (n = 3-4 biological replicates), with data analyzed by Student's *t*-
761 test; *p < 0.05, NS = not significant. **(C)** Immunoblot analysis of anti-NS4A
762 immunoprecipitated extracts or whole cell lysate (WCL) from 293T cells transfected with
763 the indicated HCV proteins (genotype 1B) or vector (V). Panels are representative of three
764 independent experiments.

765

766 **Figure 2. RIG-I deletion in Huh7 cells does not restore HCV NS4A Y16F replication.**

767 Huh-7.5 cells **(A)** or Huh7 cells **(B)** were infected with HCV, WT or NS4A Y16F (JFH1,
768 MOI 0.3). Immunoblot analysis was performed on lysates extracted at the indicated hours
769 post infection (hpi) or mock (M). Graphs next to each blot (here, and in **(E)**) show
770 quantification of NS5A protein relative to Tubulin at 72 hpi (mean \pm SEM; n = 3 biological

771 replicates). **(C)** Immunoblot of extracts of Huh7 and Huh7-RIG-I KO cells that were mock-
772 or Sendai virus (SV)-infected (20 h). **(D)** IFN- β promoter reporter luciferase expression of
773 Huh7 and Huh7-RIG-I KO cells expressing either vector or full-length RIG-I that were
774 either mock- or SV-infected (20 h). Values show the mean \pm SD (n = 3 technical
775 replicates) in relative luciferase units (RLU). **(E)** Huh7-RIG-I KO cells were infected with
776 HCV, WT or NS4A Y16F (JFH1, MOI 0.3). Immunoblot analysis was performed on lysates
777 extracted at the indicated times or mock (M). **(F-H)** Focus forming assay of supernatants
778 harvested from Huh-7.5 **(F)**, Huh7 **(G)**, and Huh7-RIG-I KO **(H)** cells at 72 hpi (MOI 0.3).
779 Data are presented as the percent HCV titer from Y16F relative to the WT (set at 100%)
780 and show the mean \pm SEM (n = 3 biological replicates). Data were analyzed by Student's
781 *t*-test; * $p < 0.05$, ** $p < 0.01$, *** $p < 0.005$, NS = not significant.

782

783 **Figure 3. HCV NS3-NS4A Y16F retains the ability to cleave MAVS.**

784 **(A)** Immunoblot analysis of lysates harvested from Huh7 cells expressing NS3-NS4A
785 (WT, Y16F, or SA (NS3 active site mutant S139A)) and vector (V) or Flag-MAVS. Arrows
786 indicate the full-length (FL) and cleaved (C) forms of MAVS. **(B)** Immunoblot analysis of
787 lysates harvested at 72 hpi from Huh-7.5 or Huh7 cells that were either mock-infected (M)
788 or infected with HCV, WT or NS4A Y16F (JFH1, MOI 0.3). Arrows indicate the full-length
789 (FL) and cleaved (C) forms of MAVS. Immunoblots are representative of three
790 independent experiments.

791

792 **Figure 4. IRF3 deletion in Huh7 cells restores HCV Y16F replication to the levels of**
793 **HCV WT.**

794 **(A)** Immunoblot of extracts of Huh7 and Huh7-IRF3 KO cells. **(B)** IFN- β promoter reporter
795 luciferase expression of Huh7 and Huh7-IRF3 KO cells expressing either vector or full-
796 length IRF3 that were either mock- or SV-infected (20 h). Values show the mean \pm SD (n
797 = 3 technical replicates). in relative luciferase units (RLU). **(C)** Immunoblot analysis of
798 lysates harvested at 72 hpi from Huh7 and Huh7-IRF3 KO cells infected with HCV, WT
799 or NS4A Y16F (JFH1, MOI 0.3). Graphs below each blot show quantification of NS5A
800 protein relative to GAPDH (mean \pm SEM; n = 3 biological replicates). **(D)** Focus forming
801 assay of supernatants harvested at 72 hpi from Huh7 or Huh7-IRF3 KO cells infected with
802 HCV, WT or NS4A Y16F (MOI 0.3). Data are presented as the percent of HCV titer from
803 Y16F relative to WT (set at 100%) and show the mean \pm SEM (n = 2 biological replicates).
804 Data were analyzed by Student's *t*-test; **p* < 0.05, ***p* < 0.01, ****p* < 0.005, NS = not
805 significant.

806

807 **Figure 5. HCV NS3-NS4A Y16F does not block IRF3 activation.**

808 **(A)** Confocal micrographs of Huh7 cells expressing GFP-IRF3 (green) and either NS3-
809 NS4A WT or Y16F (genotype 1B), or vector, that were either mock- or SV-infected (20 h)
810 and immunostained with anti-NS4A (red) or anti-SV (magenta). Nuclei were stained with
811 Hoescht (blue). Scale bar: 10 μ m. **(B)** Quantification of the percent of cells both
812 expressing GFP-IRF3 and positive for SV. Data are displayed as mean \pm SEM (n = three
813 biological replicates of 50-100 cells counted in each condition and replicate). Data were
814 analyzed by one-way ANOVA; ****p* < 0.005. **(C)** Immunoblot analysis of lysates from Huh7
815 (-), Huh7-HP WT replicon, or Huh7-HP Y16F replicon cells, and a heatmap (below) that
816 shows the mean relative fold induction (SV-infected/mock-infected, relative to *HPRT1*) of

817 specific genes as measured by RT-qPCR analysis of RNA from mock- or SV-infected (20
818 h) Huh7, Huh7-HP WT replicon, or Huh7-HP Y16F replicon cells from three biological
819 replicates. **(D)** Confocal micrographs of Huh7 and Huh7-RIG-I KO cells expressing GFP-
820 IRF3 (green) that were either mock- or SV-infected (20 h) and immunostained with anti-
821 SV (magenta). Nuclei were stained with Hoescht (blue). Scale bar: 10 μ m. Graph shows
822 the quantification of the percent of cells both expressing GFP-IRF3 and positive for SV.
823 Data are displayed as mean \pm SEM (n = three biological replicates of 50-100 cells counted
824 in each condition and replicate) and were analyzed by Student's *t*-test; *p < 0.05 and ***p
825 < 0.005.

826

827

828 **Figure 6. Over-expression of Riplet reduces HCV NS4A Y16F replication in Huh-7.5**
829 **cells.**

830 **(A)** *RNF135* (Riplet) expression relative to *GAPDH* from Huh7, Huh-7.5, and Huh-7.5 +
831 Riplet-V5 cells, as analyzed by RT-qPCR, with data displayed as mean \pm SD (n = 2-3
832 technical replicates). Data were analyzed by one-way ANOVA analysis across the means
833 of the three groups. **(B)** Immunoblot analysis of lysates harvested from the indicated cell
834 lines infected with HCV, WT or NS4A Y16F (JFH1, MOI 0.3), or mock-infected (M), at 72
835 hpi. Two different exposures (Light and Dark) are shown for NS5A. Graphs below each
836 blot show mean \pm SEM (n= 3 biological replicates) of quantification of NS5A protein
837 relative to Tubulin. **(C)** Focus forming assay of supernatants harvested at 72 hpi from the
838 indicated cell lines infected with HCV, WT or NS4A Y16F (MOI 0.3). Data are presented
839 as the percent HCV titer from Y16F relative to the WT (set at 100%) and show the mean

840 \pm SEM (n = 3 biological replicates). Data were analyzed by Student's *t*-test; *p < 0.05, **p
841 < 0.05, ***p < 0.005, NS = not significant.

842

843 **Figure 7. HCV NS4A interaction with Riplet is reduced with Y16F mutation.**

844 **(A)** Confocal micrographs of Huh7 cells expressing HA-Riplet and either NS3-NS4A WT
845 or Y16F (genotype 1B), or vector, that were immunostained with anti-NS4A (green) and
846 anti-HA (red), with the nuclei stained with Hoescht (blue). Zoom panel is taken from the
847 images in the white boxes. Images are representative of ~50 cells analyzed. Scale bar:
848 10 μ m. **(B)** Immunoblot analysis of anti-HA (NS4A) immunoprecipitated extracts or whole
849 cell lysate (WCL) from Huh7 cells transfected with plasmids expressing Flag-Riplet and
850 NS4A-HA (genotype 1B) WT or Y16F, or vector (-). The graph directly below shows the
851 mean \pm SEM (n = 3 biological replicates) of the relative fold change of Flag-Riplet to
852 NS4A-HA in the immunoprecipitated lanes. Data were analyzed by Student's *t*-test; *p <
853 0.05.

854

Figure 1

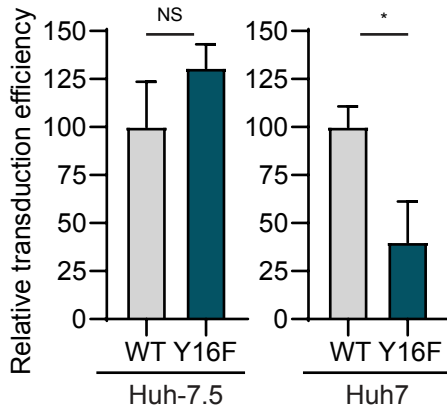
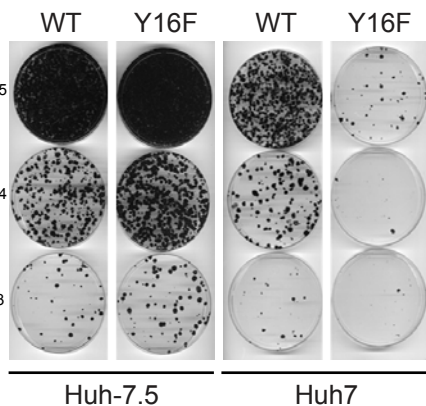
A

1662 1682 NS3 1693 1715
 1 Transmembrane 21 Interaction 32 C-terminal Domain 54
 N-STWVLAGGVLA^{AA}Y^{*}CLATGCVSII^GR^LH^VN^QR^VVV^VAPDKEVLYEAFDEMEEC-C

1 21

JFH1 (2A)	S	T	W	V	L	A	G	G	V	L	A	A	V	A	A	Y	C	L	A	T	G
H77 (1A)	V	L	S	.
Con1 (1B)	V	L	T	.
J6 (2A)
J8 (2B)	.	S
NZL1 (3A)	L	L	S	V	.
ED43 (4A)	V	L	S	V	.
EUH1480 (5A)	V	.	.	V	.	.	L	T	V	.
EUHK2 (6A)	V	L	S	V	.
QC69 (7A)	I	V	M	S	.
GT8 (8)	L	.	L	L	S	V	.

B



C

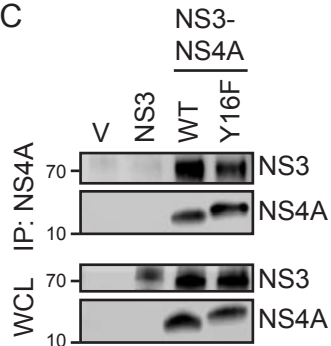


Figure 2

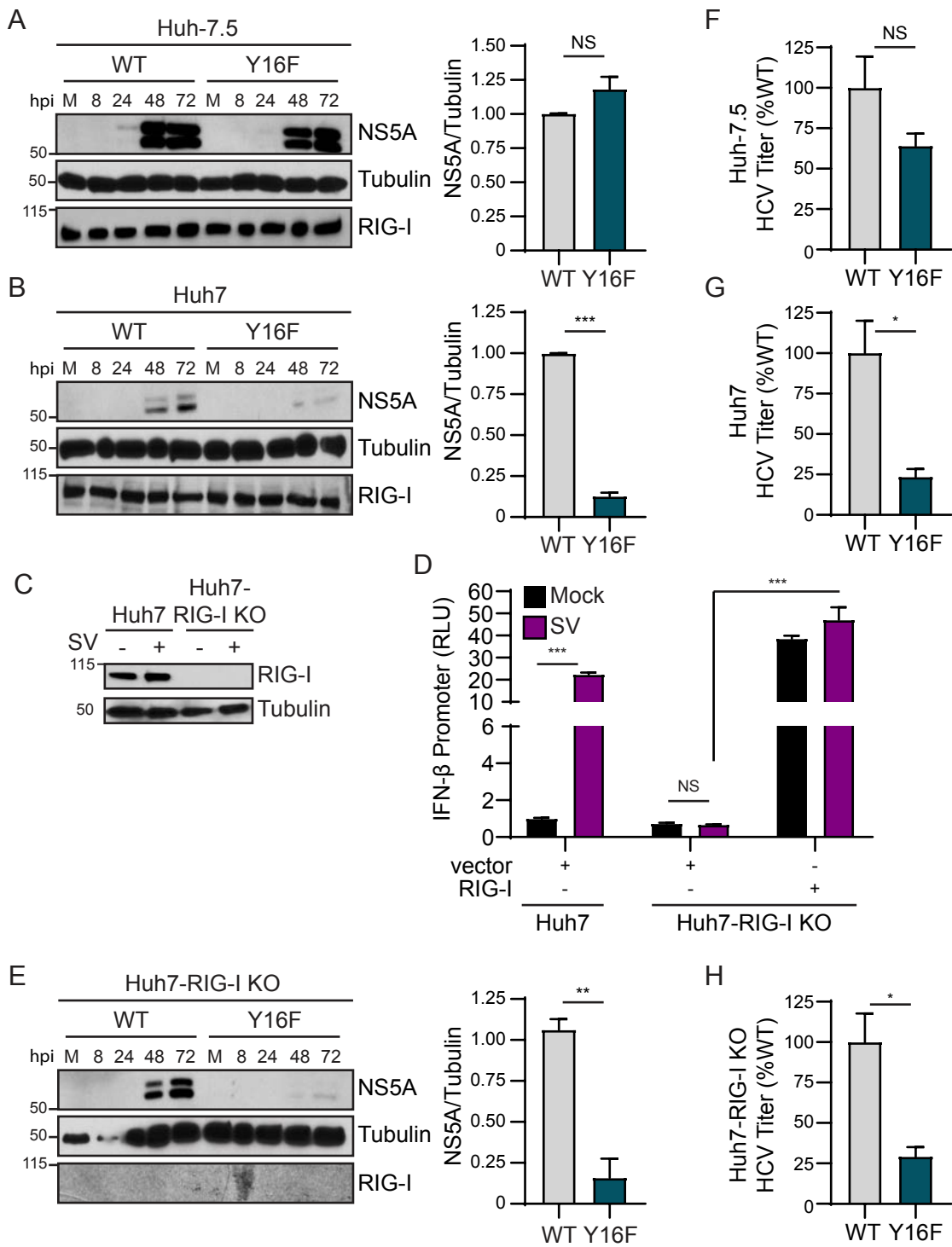


Figure 3

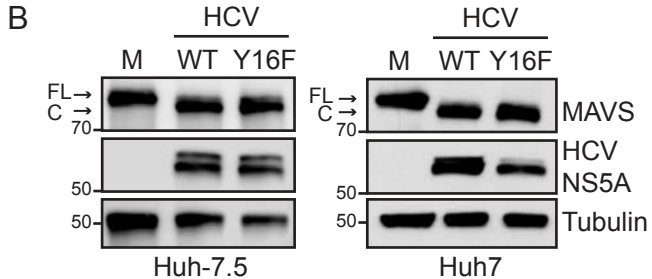
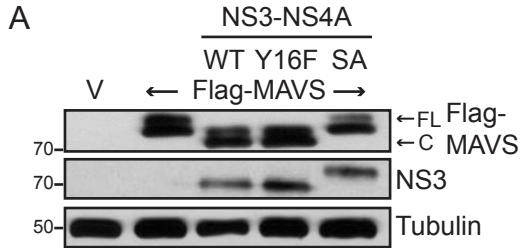
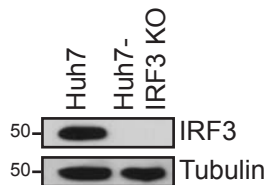
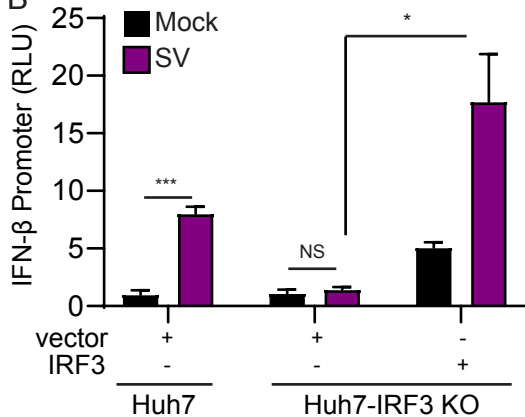


Figure 4

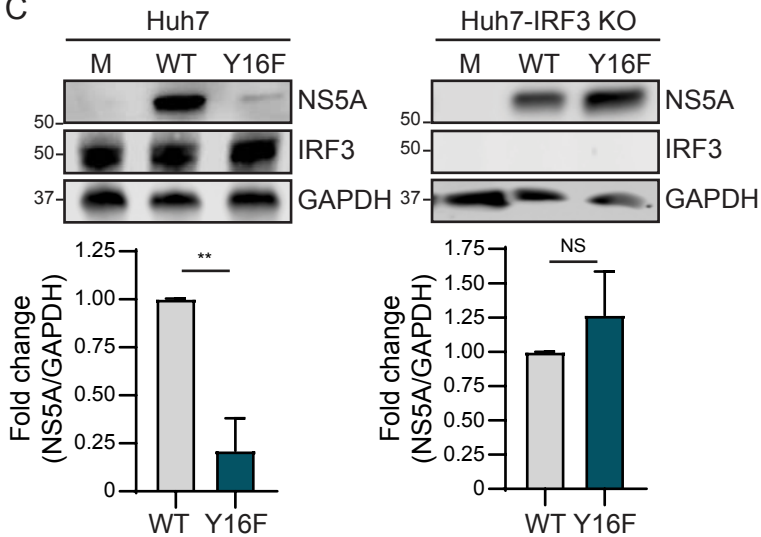
A



B



C



D

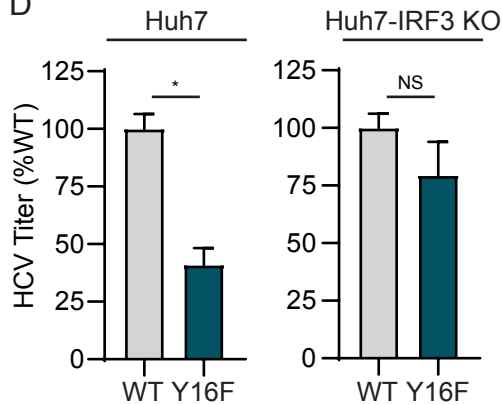
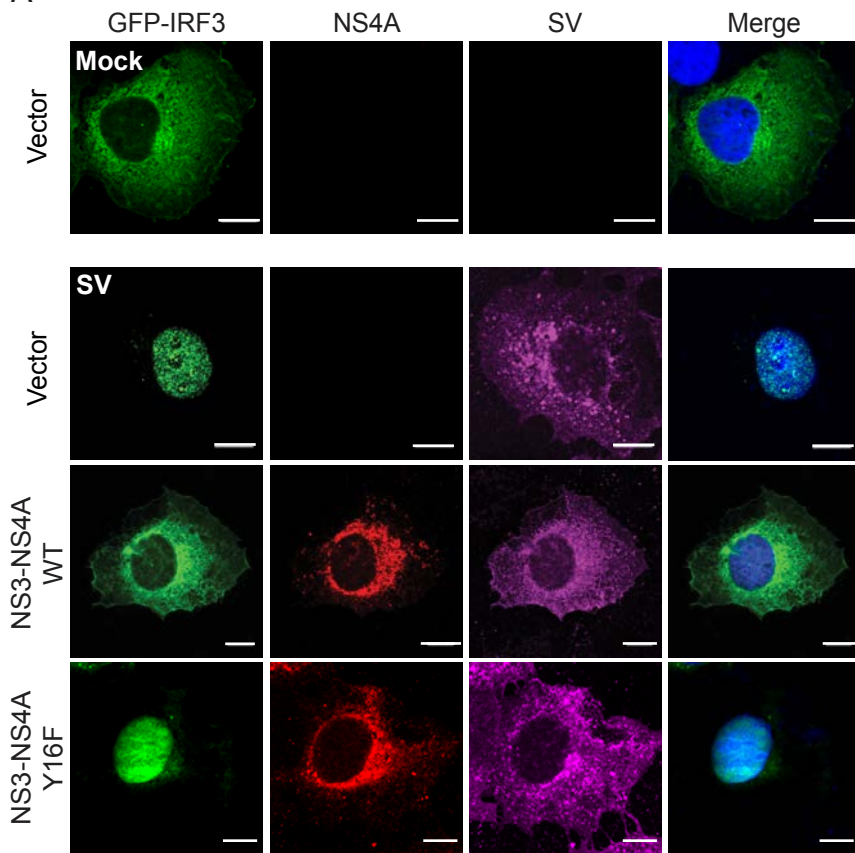
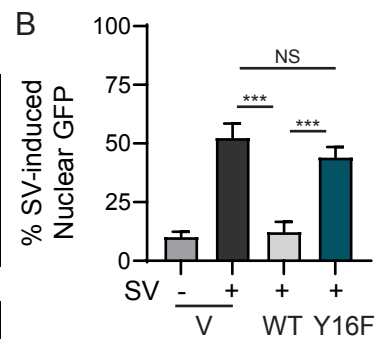


Figure 5

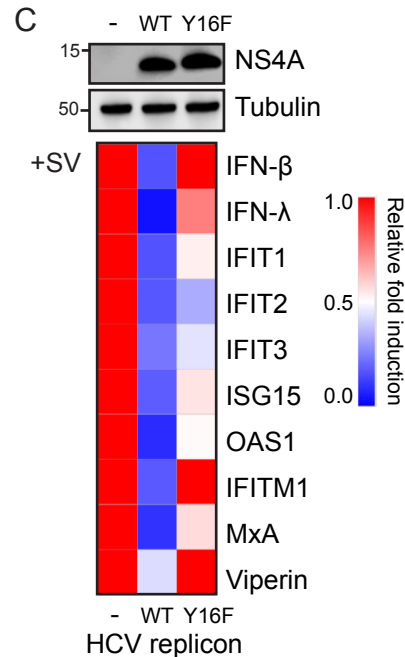
A



B



C



D

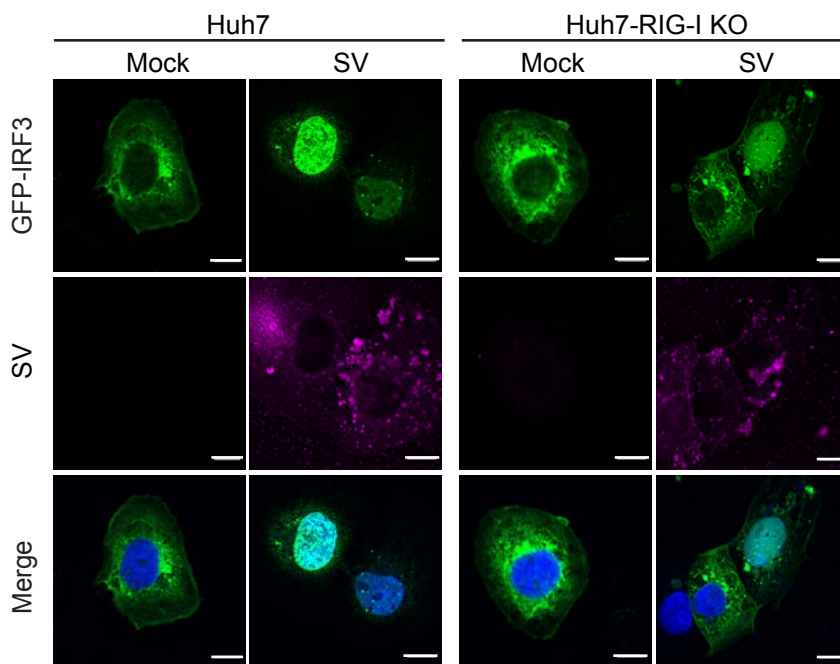


Figure 6

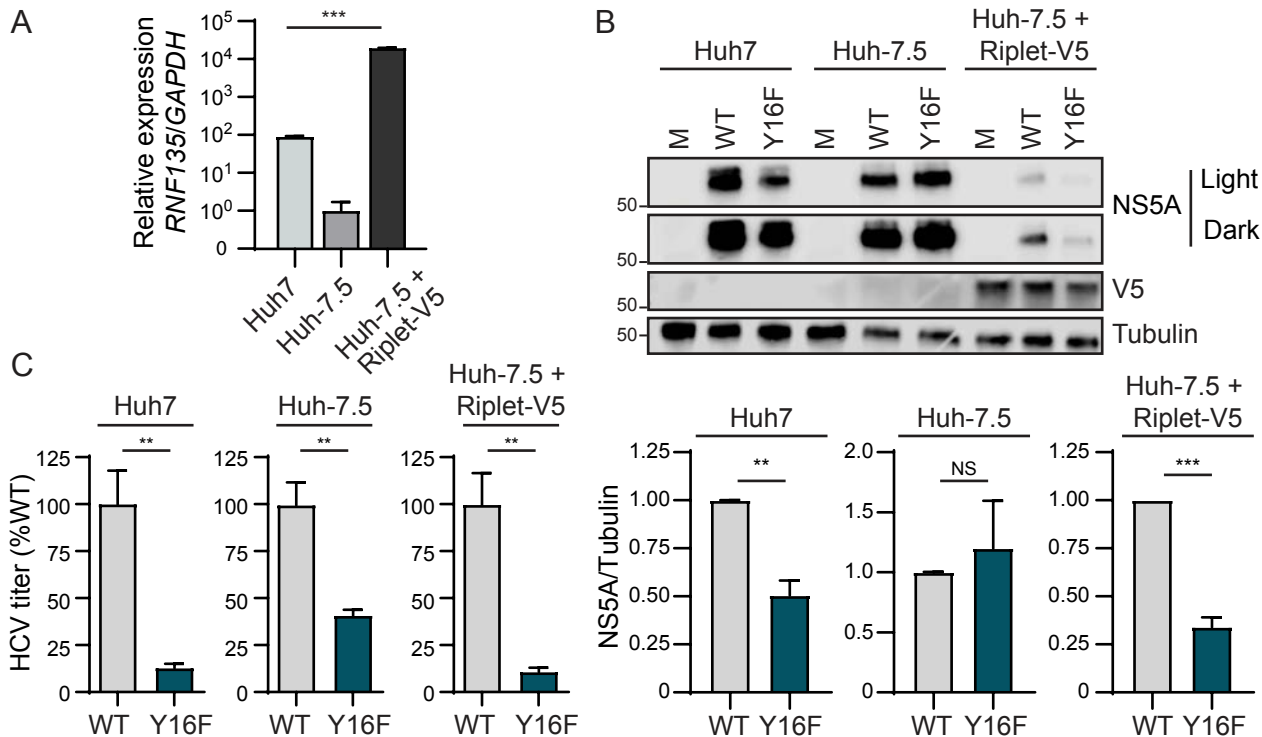


Figure 7

